

**Acetic acid on silicon (001): An exercise in chemical analogy**O. Warschkow,<sup>1,\*</sup> D. R. Belcher,<sup>2</sup> M. W. Radny,<sup>2,3</sup> S. R. Schofield,<sup>4,5</sup> and P. V. Smith<sup>2</sup><sup>1</sup>*Centre for Quantum Computation and Communication Technology, School of Physics, The University of Sydney, Sydney NSW 2006, Australia*<sup>2</sup>*School of Mathematical and Physical Sciences, The University of Newcastle, Callaghan 2308, Australia*<sup>3</sup>*Institute of Physics, Poznan University of Technology, Poznan, Poland*<sup>4</sup>*London Centre for Nanotechnology, University College London, London WC1H 0AH, United Kingdom*<sup>5</sup>*Department of Physics and Astronomy, University College London WC1E 6BT, United Kingdom*

(Received 22 July 2011; revised manuscript received 9 September 2011; published 4 October 2011)

Using the acetic acid/Si(001) system as an illustrative example, we discuss the limits and opportunities of “chemical analogy” as a paradigm to rationalize chemisorption processes on surfaces. Recent proposals that acetic acid chemisorption results in a bidentate, single-dehydrogenated product are based on earlier findings for the acetic acid/Ge(001) system. In contrast, the well-characterized reaction of acetone with Si(001) suggests that acetic acid chemisorption leads to the loss of two hydrogen atoms from the molecule. Density-functional calculations resolve this ambiguity, finding the latter structure model to be thermodynamically preferred and kinetically viable.

DOI: [10.1103/PhysRevB.84.153302](https://doi.org/10.1103/PhysRevB.84.153302)

PACS number(s): 68.43.Bc, 68.47.Fg

**I. INTRODUCTION**

Chemical analogy is widely used as a paradigm to predict the likely products of a chemical reaction. Arguments by analogy are based on the empirical principle that molecules that share certain similarities in their electronic structure are likely to follow similar patterns of reactivity. Well familiar are the chemical trends along the columns of the Periodic Table where elements share a common valence electron configuration. Central to the discipline of organic chemistry is the concept of a functional group: a subset of atoms in a larger molecule associated with a well established set of reaction patterns. Isoelectronicity and isolobality<sup>1</sup> are two of the more generalized measures of similarity that refer to, respectively, the occupation and shape of the molecules’ frontier orbitals; it is these orbitals that typically govern the course of a chemical reaction.<sup>2</sup> Along such conceptual lines, predictions of reactivity are made by reference to other systems that are sufficiently similar to the case at hand. It should be clear that such predictions are not without ambiguity. Especially in situations where general reaction patterns are still being established, choosing the “correct” analogy amongst competing proposals can be a problem. Invariably, some form of validation is required to confirm that an analogy applies.

The reaction of acetic acid (CH<sub>3</sub>COOH) with the silicon (001) surface<sup>3–7</sup> provides an excellent example. Recent scanning tunneling microscopy (STM) experiments by Shimomura *et al.*<sup>6</sup> reveal a prominent chemisorption feature that exhibits a bright protrusion centered on a surface Si–Si dimer. The authors attribute these “on-top” features to the bidentate structure shown in Fig. 1(a), which we will refer to here as acetic acid (aa) species C2 (or, aa-C2, in short). In this structure, a single hydrogen atom has detached from the molecule to form a Si–Si–H hemihydride on one surface dimer. The residual CH<sub>3</sub>COO molecular fragment is attached to a second dimer via two Si–O bonds (see also Ref. 7 wherein a similarly fragmented structure is proposed). Shimomura *et al.*<sup>6</sup> plausibly motivate their assignment using chemical analogy, noting that the same species was observed by

Hwang *et al.*<sup>8</sup> on the valence-isoelectronic Ge(001) surface. The acetic acid/Ge(001) assignment in turn is based on earlier density functional theory (DFT) calculations<sup>9</sup> that identify the aa-C2 species to be the most stable configuration on Ge(001), amongst a large set of plausible structures tested. Further support for these assignments is provided by Tersoff-Hamann<sup>10</sup> image simulations, which reproduce the dimer-centered protrusion seen in STM experiments.<sup>6,8,9</sup>

In this Brief Report, we advance an alternative structure model that is based on a competing chemical analogy. Acetone (CH<sub>3</sub>COCH<sub>3</sub>) is isoelectronic to acetic acid and also forms on Si(001) a distinct dimer-centered STM feature.<sup>11</sup> This species was attributed<sup>12</sup> in part to the acetone (ac) structure ac-D4, which is shown in Fig. 1(b) and characterized by a bidentate CH<sub>2</sub>COCH<sub>2</sub> fragment on one dimer and *two* hydrogen atoms on the adjacent dimer. By analogy, this suggests that the singly dehydrogenated structure model for acetic acid advanced in Ref. 6 falls one reaction step short of the true end product of chemisorption on Si(001): a doubly dehydrogenated bidentate that is shown as structure aa-D4 in Fig. 1(c).

**II. COMPUTATIONAL METHODOLOGY**

*Adsorption energies.* Energies of adsorption and activation energies are calculated using a procedure that we refer to as a *cluster compound model*,<sup>12,13</sup> which has a solid track record<sup>14,15</sup> of describing processes of molecular dissociation on the Si(001) surface. This approach provides a good estimate of hybrid-DFT (B3LYP; Ref. 16) adsorption energies for a large, four-dimer Si<sub>53</sub>H<sub>44</sub> surface cluster model and a 6-311(++)G(2df,2pd) basis set. The direct, “all-in-one” evaluation of energies at this level of theory is computationally prohibitive in practice; however, a good and economic approximation can be obtained by starting with a small cluster (here, two-dimer Si<sub>15</sub>H<sub>16</sub>) and a small basis set,<sup>17</sup> and correcting the results using additional *contributor calculations* that separately probe for the effects of increases in cluster size, basis set size, and level of DFT exchange–correlation. All

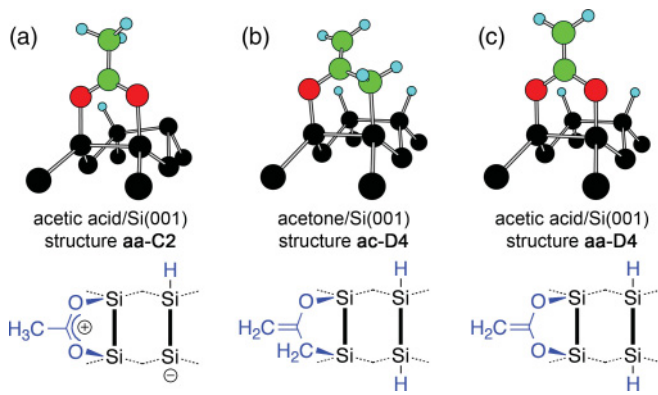


FIG. 1. (Color online) Perspective view and schematic valence structure diagram of the on-top structure aa-C2 (a) proposed in Ref. 6 to be the stable chemisorption product of acetic acid on Si(001). Comparison with the ac-D4 structure (b) observed for acetone/Si(001) suggests aa-D4 (c) as an alternative structure model of acetic acid chemisorption.

energies and activation energies reported include a vibrational zero-point correction. The full details of this approach as deployed here for the Si(001) surface are given in Ref. 12. For the Ge(001) surface, we use exactly the same approach except that four-dimer  $\text{Ge}_{53}\text{H}_{44}$  and two-dimer  $\text{Ge}_{15}\text{H}_{16}$  clusters are used in place of the silicon clusters. We note that the positions of all atoms are optimized in our calculations, except for the cluster-terminating hydrogen atoms, which are held fixed in order to emulate the strain imposed by the surrounding crystal.<sup>18</sup> All energy, geometry, and transition state calculations that contribute toward the compound model energy are performed using the GAUSSIAN 09 software.<sup>19</sup>

In order to place this method in context, we compare in Table I the calculated energy for seven acetic acid structures on Si(001)/Ge(001) with results reported by others.<sup>3,4,7-9,20</sup> Considerable differences in the results of these studies are evident in Table I, which should not be a surprise, considering the variety of computational methods used (see, e.g., Ref. 13). Our results are in best agreement with those reported by Ebrahimi *et al.*<sup>7</sup> for Si(001) and Filler *et al.*<sup>20</sup> for Ge(001),

which is presumably due to the fact that all three works are based on the hybrid, nonlocal B3LYP density functional. One difference in detail regards the relative stability of structures aa-C1 and aa-C2: Ebrahimi *et al.*<sup>7</sup> find the former structure—an end-bridge, 90°-rotated variant of structure aa-C2 [Fig. 1(a)]—to be preferred, in disagreement with our results and those of Shimomura *et al.*<sup>6</sup> Trial calculations suggest that this occurs because no structure constraints were applied to the clusters used in Ref. 7 (see Ref. 18). Comparisons with the results of Kim and Cho<sup>3</sup> and Hwang and co-workers<sup>8,9</sup> reveal larger differences, but broadly similar trends, in line with the use of local functionals in these works (generalized gradient and local-density approximation, respectively). Significant differences to the results reported by Carbone and Caminiti<sup>4</sup> are almost certainly due to the fact that these authors use a  $(2 \times 2)$  surface unit cell in conjunction with  $\Gamma$ -point-only sampling of the Brillouin zone, which is a severe approximation. Finally, Shimomura *et al.*<sup>6</sup> report energies for three structures (aa-B1, aa-C1, and aa-C2, labeled MD1, EB, and OT, respectively, in Ref. 6) not as adsorption energies, but as relative energies with respect to aa-C2. Their values of 0.71 and 0.24 eV for aa-B1 and aa-C1 are in qualitative agreement with our results of 0.27 and 0.15 eV, respectively. Given in brackets in Table I are our calculated adsorption energies with the vibrational zero-point energy contribution removed. This shows that zero-point effects account here for between  $-0.16$  and  $+0.06$  eV of the adsorption energy, which is broadly in line with other studies of Si(001) chemisorption (e.g., Ref. 13).

*Tersoff-Hamann image simulation.* Simulated STM images are calculated here using a plane-wave/pseudopotential approach to DFT as implemented in the VASP software.<sup>21,22</sup> In this approach, the Si(001) surface is represented using a periodic slab of four atomic layers thickness, which is terminated on the bottom side using hydrogen atoms. A single acetic acid molecule is placed into a  $p(4 \times 4)$  surface supercell of eight Si-Si dimers in two rows. Electron exchange and correlation are treated in the generalized gradient approximation (PW91 functional; Ref. 23), core levels are represented using ultrasoft pseudopotentials,<sup>24,25</sup> and Brillouin-zone integrations are performed using a  $2 \times 2 \times 1$   $\mathbf{k}$ -point mesh. The simulated

TABLE I. Calculated adsorption energies for selected chemisorption structures of acetic acid on Si(001) and Ge(001), comparing the results of this work with available data in the literature. Structures aa-A1, aa-B2, aa-C2, and aa-D4 are as defined in Fig. 2(b) and occur along our proposed dissociation path. Structure aa-B1 is an on-dimer variant of structure aa-B2 with the dissociated H atom bonded to the same dimer as the molecular fragment. Structure aa-B3 is a  $[2 + 2]$  cycloaddition product between the carbonyl group of acetic acid and a surface dimer. Structure aa-C1 is the end-bridge (i.e., 90°-rotated) variant of structure aa-C2, with the molecular fragment bridging between two adjacent dimers. Energies given in brackets refer to our compound model energies without the vibrational zero-point correction.

Surface	Reference	aa-A1	aa-B1	aa-B2	aa-B3	aa-C1	aa-C2	aa-D4
Si(001)	this work	-1.14	-2.58	-2.36	-0.97	-2.70	-2.85	-3.54
		(-1.10)	(-2.53)	(-2.33)	(-1.03)	(-2.66)	(-2.83)	(-3.43)
	Ref. 7		-2.56		-0.96	-2.91	-2.72	
	Ref. 4		-0.83				-1.93	
Ge(001)	Ref. 3	-0.73	-2.26		-1.08			
	this work	-0.65	-1.47	-1.06	+0.04	-1.45	-1.70	-1.09
		(-0.67)	(-1.39)	(-0.99)	(+0.02)	(-1.37)	(-1.65)	(-0.93)
	Ref. 20	-0.72	-1.71		-0.03	-1.62		
	Refs. 8 and 9	-1.37	-1.70	-1.64	-1.28	-2.10	-2.39	

filled-state STM images reported herein are calculated using the Tersoff-Hamann<sup>10</sup> approximation; that is, the tunneling current is assumed to be proportional to the density of states integrated over a small interval (here, 1 eV) below the Fermi level. Emulating a constant-current STM image, the gray scale in our simulated images represents the vertical height profile that traces a constant value of the integrated density of states (here,  $2.3 \times 10^{-3} e/\text{\AA}^3$ ). In addition, we have averaged these images over two alternating buckling configurations of the free surface dimers in order to emulate the thermal averaging that typically occurs in room-temperature experiments.

### III. RESULTS

*Acetic acid versus acetone on Si(001).* Acetic acid, acetamide ( $\text{CH}_3\text{CONH}_2$ ), and acetone form an isoelectronic sequence of compounds that have in common the acetyl fragment ( $-\text{COCH}_3$ ) and differ in the acetyl residue, being hydroxyl ( $-\text{OH}$ ), amino ( $-\text{NH}_2$ ), and methyl ( $-\text{CH}_3$ ), respectively. For acetone, theory<sup>12</sup> has resolved in great detail the full dissociation mechanism that gives rise to three observable intermediates in STM experiments.<sup>11</sup> Relevant to the discussion here is the reaction channel shown in Fig. 2(a) that leads to the dimer-bridge dissociated structure ac-D4, which is observed as the dimer-bridge (DB) feature. This channel goes through four discrete steps: adsorption and first molecule-surface bond formation (free surface  $\rightarrow$  ac-A1), first proton transfer (ac-A1  $\rightarrow$  ac-B2), second molecule-surface bond formation (ac-B2  $\rightarrow$  ac-C2), and second proton transfer (ac-C2  $\rightarrow$  ac-D4). All four steps present low activation barriers ( $E_A < 0.4$  eV) and thus the direct path to structure ac-D4 proceeds very rapidly. The only kinetic holdup occurs for some acetone molecules that are diverted into another reaction channel (not shown here) leading to a metastable  $[2 + 2]$  cycloaddition product.<sup>12,26-30</sup>

We postulate here that the dimer-centered feature observed by Shimomura *et al.*<sup>6</sup> for acetic acid is formed by a chemically analogous pathway. This path is shown in Fig. 2(b) and it is nominally derived from the acetone

sequence [Fig. 2(a)] by replacing one  $\text{CH}_x$  fragment ( $x = 2, 3$ ; red color symbols) with an isovalent  $\text{OH}_{x-2}$  fragment containing two fewer hydrogen atoms. Despite the *ad hoc* nature of this substitution, the resulting path remains plausible overall: the two molecule-surface bond formation steps (free surface  $\rightarrow$  aa-A1 and aa-B2  $\rightarrow$  aa-C2) bring together a carbonyl oxygen with a down-buckled silicon dimer end, just as seen in the initial adsorption step for acetone. The two deprotonation reactions (aa-A1  $\rightarrow$  aa-B2 and aa-C2  $\rightarrow$  aa-D4) should also occur readily because acetic acid is the stronger acid. Note also that the structure proposal of Shimomura *et al.*,<sup>6</sup> structure aa-C2, occurs as an intermediate in this path, being the direct analog to the short-lived species ac-C2 in the acetone path.

*Comparative energetics.* Quantitative backup to these arguments is provided by DFT calculations. Computed adsorption energies for the sequence of structures A1 to D4 are plotted in Fig. 3(a) for acetic acid and acetone on Si(001) as well as acetic acid on Ge(001). The comparison of these energies illustrates the relative performance of acetic acid/Ge(001) and acetone/Si(001) as analogous model systems for acetic acid/Si(001). Across the series, the energies of acetic acid/Si(001) are closer to those of acetone/Si(001) than to acetic acid/Ge(001). More importantly, we can see for the two Si(001) systems that each step along the path leads to a gain in energy such that the final structure D4 is the most stable. This is very different for acetic acid on Ge(001), which follows the qualitative energetics on Si(001) only up to the aa-C2 stage. In the last step, the two surfaces diverge sharply with structure aa-D4 being significantly (0.6 eV) less stable on Ge(001) than structure aa-C2. Thus, while our results support the earlier Hwang *et al.*<sup>8</sup> assignment of structure aa-C2 to the acetic acid/Ge(001) chemisorption product, this support does not extend to the model by Shimomura *et al.*<sup>6</sup> Clearly, structure aa-C2 is not the thermodynamic end product of acetic acid chemisorption on Si(001).

*Kinetics.* The thermodynamic stability of structure aa-D4 alone, however, does not imply that this species is formed, because kinetics is a governing factor for many

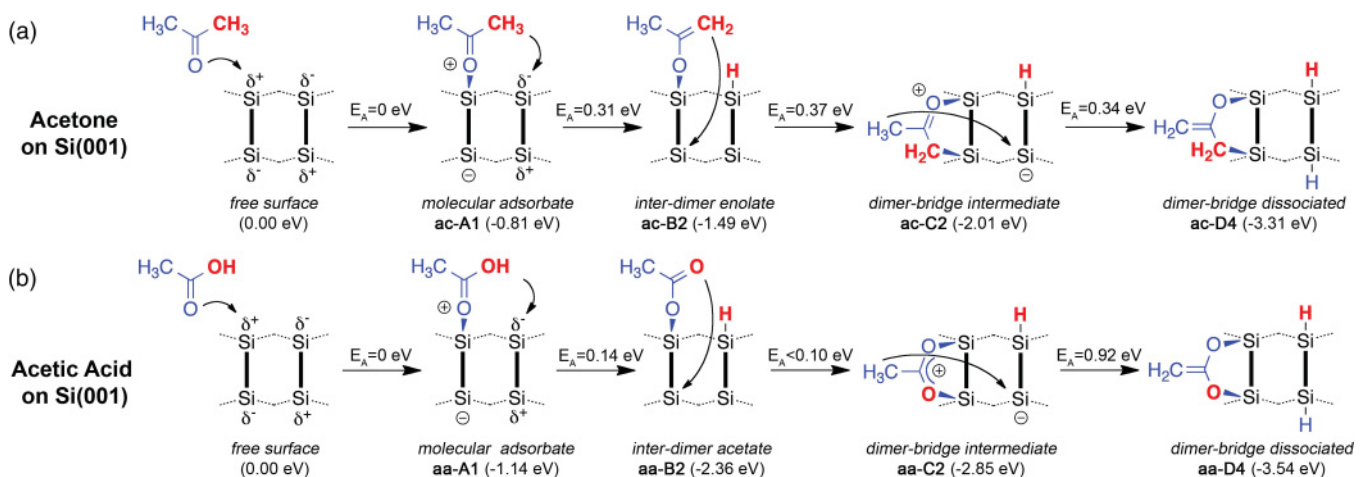


FIG. 2. (Color online) Schematic valence structure diagrams outlining (a) the reaction channel for acetone on Si(001) that leads in four steps to the dimer-bridge dissociated structure ac-D4 (see Ref. 12 for details), and (b) the chemically analogous path for acetic acid on Si(001). Calculated adsorption energies are included with each structure as are the activation energies of reaction,  $E_A$ , between them.

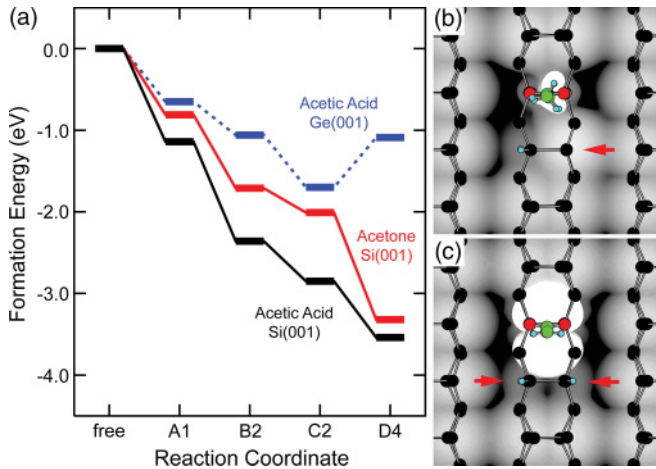


FIG. 3. (Color online) (a) Comparative energetics along the four step dissociation path (cf. Fig. 2) leading to the dimer-bridge dissociated structures ac/aa-D4. (b),(c) Tersoff-Hamann simulated filled-state STM images for the two Si(001) acetic acid chemisorption structures aa-C2 (b) and aa-D4 (c). The images are averaged over two alternating buckling configurations of the surrounding free dimers to emulate the thermal averaging that occurs in experiment. The images are overlaid with structure models of these buckling configurations.

processes on Si(001). In order to illuminate this further, we have computed activation energies along our aa-A1 to aa-D2 path [see Fig. 2(b)]. Up to structure aa-C2 the barriers are very low ( $E_A < 0.2$  eV), consistent with the near-instant formation of this species at room temperature. For the aa-C2 $\rightarrow$ aa-D4 reaction we obtain an activation energy  $E_A = 0.92$  eV and a Vineyard<sup>31</sup> attempt frequency of  $A = 8 \times 10^{11}$  s<sup>-1</sup>. This barrier is considerably larger than the equivalent one for acetone ( $E_A = 0.34$  eV and  $A = 5 \times 10^{11}$  s<sup>-1</sup>), which means the formation of aa-D4 is relatively slow on STM imaging time scales (minutes per image, typically). At room temperature, the thermal Arrhenius rate computes to 0.0003 s<sup>-1</sup> per molecule; i.e., structure aa-C2 has an estimated average lifetime of approximately 1 h before dissociating into the more stable structure aa-D4. Moderately elevated temperatures of 340 and 390 K reduce the average lifetime to 1 min and 1 sec, respectively. We note in passing that an alternative chemisorption path proposed in Ref. 4 presents much higher barriers to reach structure aa-C2 and is therefore not competitive with our path.<sup>32</sup>

The larger barrier and slower rate of the acetic acid reaction in comparison to acetone can be rationalized by inspecting the three-dimensional geometry of the species involved. As illustrated in Fig. 4, the distance between the shifting hydrogen atom and the hydrogen-accepting silicon atom is a crucial determinant of the activation barrier. In the acetone intermediate ac-C2 [Fig. 4(a)], the molecular fragment is slightly angled toward the adjacent dimer, whereas the corresponding acetic acid intermediate aa-C2 [Fig. 4(b)] is not. As a result, the critical hydrogen-silicon distance is considerably shorter for acetone (3.93 Å) than for acetic acid (4.72 Å). The calculated transition states to form structures ac/aa-D4 in Figs. 4(c) and 4(d) are geometrically very similar (1.87 Å vs 1.95 Å), which means that the acetic acid transition

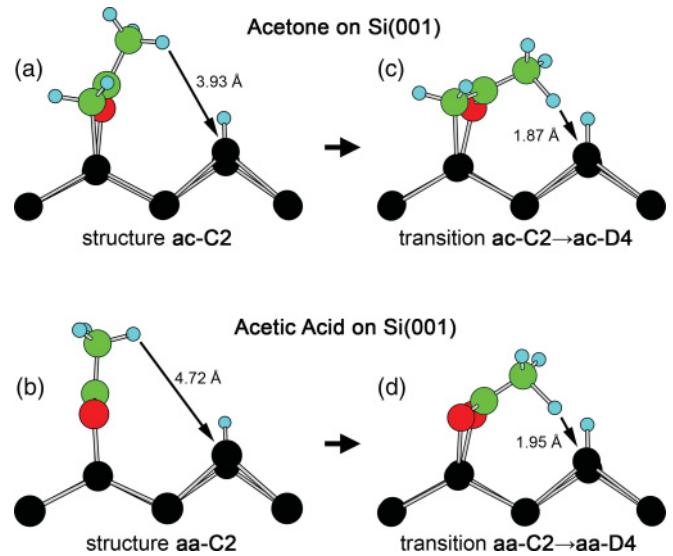


FIG. 4. (Color online) Comparative side views of structures ac/aa-C2 (a),(b) and the transition states (c),(d) leading to structures ac/aa-D4 for acetone and acetic acid on Si(001). The distance between the shifting hydrogen atom and the accepting silicon site is indicated in all four structures.

state is more distorted relative to the C2 precursor, and, consequently, less stable. The presence or absence of an angle in the molecular fragment is in turn related to the degree of planar  $sp^2$  hybridization in the five-membered ring that is formed by the three-atom bridge and the silicon dimer. In the acetone intermediate [Fig. 4(a)], the  $-CH_2-$  group is tetrahedrally  $sp^3$  hybridized, which imposes a twist on the ring and causes the molecular fragment to angle. In the acetic acid structure [Fig. 4(b)], all three bridge atoms are  $sp^2$ -hybridized, resulting in an overall planar ring structure and a fully upright orientation of the molecular fragment.

*STM appearance.* For acetic acid, the above kinetics results suggest that in room-temperature STM experiments both the metastable intermediate aa-C2 and, in time, the thermodynamic end product aa-D4 should be observable. Calculated filled-state STM images for these two species are shown in Figs. 3(b) and 3(c) to illustrate how they may be distinguished. The image simulations confirm that both structures aa-C2 and aa-D4 present a sharp protrusion that is centered above one dimer, consistent with the experimental appearance [Figs. 3(a) and 3(c) in Ref. 6]. We note that the protrusion for structure aa-D4 [Fig. 3(c)] is considerably larger than for structure aa-C2 [Fig. 3(b)], which is explained by the predominant  $\pi$  and  $\sigma$  character of the methylene ( $=CH_2$ ) and methyl ( $-CH_3$ ) groups, respectively, at the tip of the molecular fragment. In particular, the  $\pi$  character of structure aa-D4 is evident in Fig. 3(c) in a characteristic narrowing of the protrusion near the molecular plane. The predicted size of the protrusion, however, is unlikely to be useful as a distinguishing characteristic because in experiment the size/resolution of a highly protruding image feature is also dependent on the shape of the STM tip. More significant is the darker appearing dimer predicted for structure aa-D4 [arrows in Fig. 3(c)] that is a hallmark of a H-Si-Si-H monohydride. In contrast, structure aa-C2 presents on this dimer a secondary protrusion that is positioned off-center

from the dimer row [arrow in Fig. 3(b)]. This protrusion is caused by the lone-pair orbital of the Si-Si-H hemihydride. As recognized in Ref. 6, the hemihydride will induce static pinning<sup>33</sup> in the surrounding free dimers. This is confirmed by our cluster calculations: the energy difference between the two buckling configurations are 0.11 and 0.02 eV adjacent to the hemihydride and the molecular fragment, respectively. This suggests<sup>34,35</sup> for structure aa-C2 strong pinning on one side at room temperature, and weaker pinning on the other. In contrast, structure aa-D4, being symmetric about the dimer row, does not pin.

From the experimental details given in Ref. 6, the sample temperature during the acetic acid dosing was estimated at between 300 and 350 K, due to the slow rate of heat dissipation after sample flash anneal. As discussed above, time and temperature are factors that influence the kinetics; specifically, the balance of aa-C2 and aa-D4 species, and the rate of aa-C2→aa-D4 conversion. Two indicators already suggest that structure aa-D4 is responsible for at least some of the bright protrusions seen in Fig. 3(c) of Ref. 6. First, several of the adsorbate features shown exhibit a dark region on one side of the protrusion consistent with the depression seen in our calculated image for structure aa-D4 [Fig. 3(c)]. Second, the reported STM voltage bias of  $-3.5$  V and set point current of 0.3 nA are rather large, which sharply increases the probability for STM-induced reactions (see, e.g., Ref. 36). Localized heating alone, due to current-induced vibrational excitation, is likely to accelerate the dissociation of structure aa-C2 into the thermodynamic end product aa-D4. Further detailed STM experiments under carefully controlled conditions may be able to resolve the two species and directly image the transition between them.

#### IV. DISCUSSION AND CONCLUSIONS

The above analysis illustrates how chemical analogy, when backed up by targeted DFT calculations, is a powerful approach to understand organic molecule reactions on silicon surfaces. Two analogies, acetic acid/Ge(001) and acetone/Si(001), were used to “triangulate” the likely reaction product of acetic acid chemisorption on Si(001). The two analogies differ on which structure (aa-C2 or aa-D4) is the thermodynamic end product; however, this ambiguity is easily resolved by calculation of the relative energies, and the transition state between them. Somewhat conciliatory, these calculations suggest that both species are sufficiently long-lived to be observable in STM experiments.

The insights gained for acetic acid/Si(001) can in turn be put to use as an analogy for other reaction systems. For example, acetamide is in the same isoelectronic sequence as acetone and acetic acid. Since both acetic acid and acetone form bidentate chemisorption species on Si(001), we should expect acetamide (am) to do the same. Figure 5 sketches out the likely products obtained by replacing the  $\text{CH}_x/\text{OH}_{x-2}$  fragments in the acetone/acetic acid paths with isovalent  $\text{NH}_{x-1}$ . Supporting the analogy, we find the calculated energies for the am-C2 and am-D4 bidentate structures to be very close (within 0.2 eV) to those of the corresponding acetic acid species. The activation energy for the am-C2→am-D4 reaction is calculated to be 1.20 eV; thus the process will be

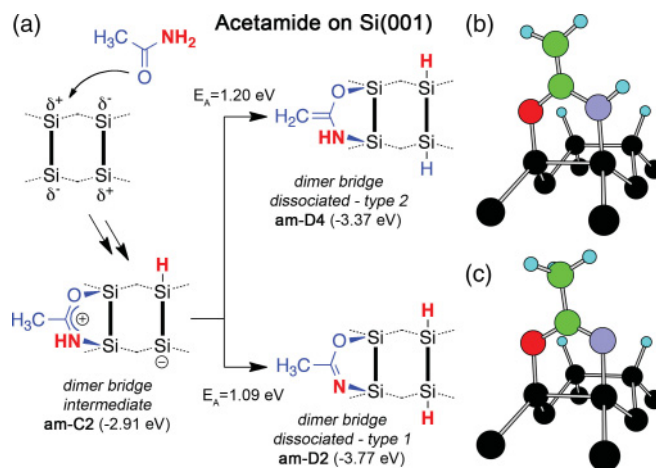


FIG. 5. (Color online) (a) Analogous to acetic acid and acetone, acetamide is expected to form bidentate chemisorption species on Si(001). The two competing end products of dissociation: (b) structure am-D4 and (c) structure am-D2.

somewhat slower than for acetic acid or acetone. Analogous to acetone (see Ref. 12), there is an alternative path from structure am-C2 in which the hydrogen atom shifts from the NH fragment in the ring instead of from the methyl group at the top. This produces structure am-D2 as shown in Figs. 5(a) and 5(c), which is 0.4 eV more stable than structure am-D4, and thus the thermodynamically preferred species (as is the case in acetone). With a slightly lower activation barrier of 1.09 eV, structure am-D2 is also kinetically preferred. The acetic acid structure aa-C2, for lack of a hydrogen atom at the O site, cannot follow this alternate path.

Taking a wider perspective, the general reaction patterns outlined here for acetyl ( $R\text{-COCH}_3$ ), amide ( $R\text{-CONH}_2$ ), and carboxyl ( $R\text{-COOH}$ ) all produce analogous bidentate linkages between an organic molecule and the Si(001) surface. This is of considerable interest in the context of molecular electronics research for at least two reasons. First, a strong bidentate attachment between surface and molecule mitigates the risk of current-induced detachment as is often observed<sup>36,37</sup> for more weakly bonded species. Second, through these reaction patterns we can create surface-molecule linkages involving various pairings of Si-N, Si-O, and Si-C bonds. Choice over the linkage group in turn affords a means to modulate the relative alignment of electronic levels between the molecular residue  $R$  and the surface. This may be exploited in the design of certain nonlinear molecular electronics properties such as negative differential resistance.

#### ACKNOWLEDGMENTS

O.W. was supported by the Australian Research Council Centre of Excellence for Quantum Computation and Communication Technology (Project No. CE11E0096). M.W.R. acknowledges the Polish Ministry of Science & Higher Education (Project No. N N202 169236) for support. S.R.S. was supported by an EPSRC Career Acceleration Fellowship (EP/H003991/1).

\*o.warschkow@physics.usyd.edu.au

- <sup>1</sup>R. Hoffmann, *Angew. Chem., Int. Ed. Engl.* **21**, 711 (1982).
- <sup>2</sup>K. Fukui, *Science* **218**, 747 (1982).
- <sup>3</sup>H.-J. Kim and J.-H. Cho, *Phys. Rev. B* **72**, 195305 (2005).
- <sup>4</sup>M. Carbone and R. Caminiti, *Surf. Sci.* **602**, 852 (2008).
- <sup>5</sup>H.-K. Lee, K.-J. Kim, J.-H. Han, T.-H. Kang, J. W. Chung, and B. Kim, *Phys. Rev. B* **77**, 115324 (2008).
- <sup>6</sup>M. Shimomura, T. K. Kawaguchi, Y. Fukuda, K. Murakami, A. Z. AlZahrani, and G. P. Srivastava, *Phys. Rev. B* **80**, 165324 (2009).
- <sup>7</sup>M. Ebrahimi, J. F. Rios, and K. T. Leung, *J. Phys. Chem. C* **113**, 281 (2009). The structure model advanced in this paper is an end-bridge oriented (i.e., 90°-rotated) variant of the on-top structure proposed in Ref. 6. This variant, however, is not compatible with the dimer-centered chemisorption feature observed in STM experiments.
- <sup>8</sup>E. Hwang, D. H. Kim, Y. J. Hwang, A. Kim, S. Hong, and S. Kim, *J. Phys. Chem. C* **111**, 5941 (2007).
- <sup>9</sup>D. H. Kim, E. Hwang, S. Hong, and S. Kim, *Surf. Sci.* **600**, 3629 (2006).
- <sup>10</sup>J. Tersoff and D. R. Hamann, *Phys. Rev. Lett.* **50**, 1998 (1983).
- <sup>11</sup>S. R. Schofield, S. A. Sarairoh, P. V. Smith, M. W. Radny, and B. V. King, *J. Am. Chem. Soc.* **129**, 11402 (2007).
- <sup>12</sup>O. Warschkow, I. Gao, S. R. Schofield, D. R. Belcher, M. W. Radny, S. A. Sarairoh, and P. V. Smith, *Phys. Chem. Chem. Phys.* **11**, 2747 (2009).
- <sup>13</sup>O. Warschkow, T. L. McDonell, and N. A. Marks, *Surf. Sci.* **601**, 3020 (2007).
- <sup>14</sup>O. Warschkow, S. R. Schofield, N. A. Marks, M. W. Radny, P. V. Smith, and D. R. McKenzie, *Phys. Rev. B* **77**, 201305(R) (2008).
- <sup>15</sup>D. R. Belcher, S. R. Schofield, O. Warschkow, M. W. Radny, and P. V. Smith, *J. Chem. Phys.* **131**, 104707 (2009).
- <sup>16</sup>A. D. Becke, *J. Chem. Phys.* **98**, 5648 (1993); C. Lee, W. Yang, and R. G. Parr, *Phys. Rev. B* **37**, 785 (1988).
- <sup>17</sup>Two combinations of atomic basis sets, *large* and *small*, are used in our compound model energy calculations. The *large* basis set is the standard 6-311G(2df, 2pd) Gaussian-type orbital set with additional “++” diffuse functions added to the atoms of the adsorbate and the Si-Si dimers at the surface. We have denoted this variation as “6-311(+++G(2df, 2pd))” in the text. The *small* basis set is composed of a 6-311(+++G(d, p) Gaussian-type orbital set for all atoms except for the silicon atom below the second (subsurface) layer and the cluster-terminating atoms, which are described using a LANL2DZ valence double- $\zeta$ /pseudopotential set. See details of basis definition in Ref. 12.
- <sup>18</sup>Structural constraints on the cluster-terminating hydrogen atoms are used as an *ad hoc* representation of the strain due to the atoms of the surface/crystal that are not explicitly represented by the cluster. Such constraints are important as they prevent the cluster from unrealistically relaxing in response to an adsorbed molecule. The positions of the cluster-terminating hydrogen atoms are determined using a relaxed slab model of a (2×1) H:Si(001) surface acting as a template. The hydrogen atoms were thus placed with a Si-H bond length of 1.49 Å along any Si-Si bond that is broken by the cluster (see Ref. 13 for details). An analogous procedure using a (2×1) H:Ge(001) template and a Ge-H bond length of 1.54 Å is used here to define the termination of the germanium clusters.
- <sup>19</sup>M. J. Frisch *et al.*, GAUSSIAN 09, Revision A.02 (Gaussian, Inc., Wallingford CT, 2009).
- <sup>20</sup>M. A. Filler, J. A. Van Deventer, A. J. Keung, and S. F. Bent, *J. Am. Chem. Soc.* **128**, 770 (2006).
- <sup>21</sup>G. Kresse and J. Hafner, *Phys. Rev. B* **47**, 558 (1993); **49**, 14251 (1994).
- <sup>22</sup>G. Kresse and J. Furthmüller, *Comput. Mater. Sci.* **6**, 15 (1996).
- <sup>23</sup>J. P. Perdew and Y. Wang, *Phys. Rev. B* **45**, 13244 (1992).
- <sup>24</sup>D. Vanderbilt, *Phys. Rev. B* **41**, 7892 (1990).
- <sup>25</sup>G. Kresse and J. Hafner, *J. Phys.: Condens. Matter* **6**, 8245 (1994).
- <sup>26</sup>J. A. Barriocanal and D. J. Doren, *J. Am. Chem. Soc.* **123**, 7340 (2001).
- <sup>27</sup>G. T. Wang, C. Mui, C. B. Musgrave, and S. F. Bent, *J. Phys. Chem. B* **105**, 12559 (2001).
- <sup>28</sup>C. Hamai, A. Takagi, M. Taniguchi, T. Matsumoto, and T. Kawai, *Angew. Chem., Int. Ed. Engl.* **43**, 1349 (2004).
- <sup>29</sup>J.-H. Lee, J. Y. Lee, and J.-H. Cho, *J. Chem. Phys.* **129**, 194110 (2008).
- <sup>30</sup>Our calculations suggest that the [2 + 2] cycloaddition product for acetic acid (structure aa-B3 in Table I) is very short-lived on Si(001), being 0.17 eV *less* stable than its precursor, the molecular adsorbate aa-A1. Thus the [2 + 2] species should not occur in the STM images of Ref. 6.
- <sup>31</sup>G. H. Vineyard, *J. Phys. Chem. Solids* **3**, 121 (1957).
- <sup>32</sup>In the reaction path proposed by Carbone and Caminiti,<sup>4</sup> the rate-determining step in the formation of structure aa-C2 (labeled 5 in Ref. 4) is the hydrogen-shift reaction 3 → 4 via transition state TS3 (see Figs. 1 and 3 in Ref. 4). From the data given, the activation energy of this step evaluates to 1.83 eV whereas in our path the largest activation energy is only 0.14 eV. Note further that *all* of the transition states in Ref. 4 have energies that are above the dissociation limit, which implies that acetic acid would rather detach from the surface than undergo any of these reactions.
- <sup>33</sup>R. A. Wolkow, *Phys. Rev. Lett.* **68**, 2636 (1992).
- <sup>34</sup>H. F. Wilson, N. A. Marks, and D. R. McKenzie, *Surf. Sci.* **587**, 185 (2005).
- <sup>35</sup>P. V. Smith, O. Warschkow, M. W. Radny, S. R. Schofield, and D. R. Belcher, *J. Chem. Phys.* **134**, 064709 (2011).
- <sup>36</sup>S. N. Patistas, G. P. Lopinski, O. Hul’ko, D. J. Moffatt, and R. A. Wolkow, *Surf. Sci.* **457**, L425 (2000).
- <sup>37</sup>P. Kruse and R. A. Wolkow, *Appl. Phys. Lett.* **81**, 4422 (2002).